

Cavity Search for dark-matter Axion

Author's Name

Department of Physics, University of Maryland, College Park, Maryland 20742, USA
(12 March 2007)

Many different experiments have been searching for axion-like forces and some sign of existence of the axion. The axion is a hypothetical elementary particle that would solve two major problems in science. It was originally a consequence of a solution to explain the lack of CP -violation in the physics of quarks and gluons, the fundamental constituents of objects such as protons and neutrons. Later, it was recognized to be a good dark matter candidate. Today, it remains as one of the leading dark matter candidates. The ADMX experiment is the only experiment able to probe realistic dark matter axion models with sufficient sensitivity in the expected mass regime.

I. Introduction

Axion is a hypothetical elementary particle postulated by Peccei and Quinn in 1977 to resolve the strong- CP problem in quantum chromodynamics (QCD). This theory possesses a non-trivial vacuum structure that, in principle, permits the violation of the combined symmetries of charge conjugation and parity, collectively known as CP . The effective strong CP violating parameter in the QCD Lagrangian, Θ , appears as a Standard Model (SM) input parameter that must be measured. But generic CP -violation in the strongly interacting sector would create the electric dipole moment for the neutron, while experimental constraints on neutron's dipole electric moment imply CP violation from QCD be extremely tiny, and then Θ (periodic parameter $0 < \Theta < 2\pi$) extremely small or absent; one part in 10^9 [1]. A solution for this problem is called Peccei-Quinn mechanism [2] which promotes the parameter Θ to a dynamic field by adding a new global symmetry to the SM. It becomes spontaneously broken resulting in a new particle known as axion that relaxes the CP violation parameter to zero [3].

The mass of the axion is constrained by cosmology to be larger than $1 \mu\text{eV}$ and by the neutrino signal from Supernova (1987a) to be less than 10 meV ($20 \mu\text{m} < \lambda_{\text{Axion}} < 20 \text{ cm}$, $\lambda = \hbar/mc$) and is a good cold dark matter candidate [4]. Since the axion interacts only very weakly with ordinary matter, it is very difficult to detect. Nevertheless, there are different experiments searching for the axion by very different methods. Some of them only constrain the strength of the related axion parameters and others are able to probe axion models.

There are several groups interested in the interaction associated with the exchange of a light or massless pseudoscalar Goldstone boson, or similar interactions as the axion in mass-spin interactions [5-8]. Moody and Wilczek [9] proposed an interaction potential generated by a boson with spin zero, describing these axion-like interactions:

$$V(r) = g_p^e g_s \frac{\hbar^2}{8\pi m_e} \hat{\sigma} \cdot \hat{r} \left(\frac{1}{r\lambda} + \frac{1}{r^2} \right) e^{-r/\lambda} \quad (1)$$

where g_s is the coupling strength at the scalar vertex (nucleon) and g_p^e the coupling strength at the pseudoscalar vertex (electron) [8]. If the mass of the exchange particle is m , the range of interaction is given by $\lambda = \hbar/mc$. This potential violates parity P and time reversal T . At the moment the axion is the most likely candidate particle for generating such a new interaction [8]. In the experiments searching for these kind of interactions $(g_s g_p^e)_{\text{Axion}} < 6 \times 10^{-33} \theta/\lambda^2$, where θ is constrained by experimental limits on the dipole moment on the neutron to be less than 10^{-9} [1].

A number of experiments have placed constraints on the strength $g_s g_p^e$ as a function of range testing deviations from the potential described by Eq. (1). Heckel *et al.* [5] used a torsion balance with an attached spin polarized test mass to set the strongest constraint achieved at ranges larger than 1 m. Youdin *et al.* [6] set the best constraint in the range $10 \text{ cm} < \lambda < 1 \text{ m}$, comparing the relative precession frequencies of Hg and Cs magnetometers as a function of the position of masses with respect to an applied magnetic field. Ni and his colleagues [7] used SQUID in an attempt to detect the change in polarization induced in a paramagnetic salt induced by the motion of a source mass setting the strongest constraints in the range $5 \text{ mm} < \lambda < 10 \text{ cm}$. Hammond *et al.* [8] used a spherical superconducting torsion balance with suspended test cylindrical masses and a spin source. They used a toroidal electromagnet to measure the oscillation of the torsion balance coherent with the sinusoidal current driving the spin source, setting the best constraints at a range of 1 mm. The range and sensitivity of all these experiments are far from the axion regime. Even though there is a proposal with higher sensitivity using superconductive accelerometers in a Spin-Mass Interaction Low-Temperature Experiment (SMILE) able to test some axion-like interactions near the axion regime [10].

In contrast, Sikivie devised a method to find these axions via conversion into photons within a tunable

microwave cavity threaded with a static magnetic field via Primacoff effect [11].

The conversion into microwave photons is then enhanced by the resonant cavity (with quality factor about 10^5) and the strength of the static magnetic field; the excess microwave photons above thermal background from axion conversion are detected by a low noise pre-amplifier coupled to the cavity. This excess in power constitutes the candidates for detected axions. The expected signature of the axion signal are narrow peaks of excess power at frequency $f = m_a c^2/h$ with width $\sim 10^{-6}$ due to virialized motion of galactic axions in the halo, or $\sim 10^{-11}$ due to the recent capture of extra-galactic axions by the gravitational potential of our galaxy. Then it is necessary to increase the signal-to-noise ratio of the converted axions minimizing the noise of the detectors .

II. Theory

The axions can be detected by stimulating their conversion to photons in a strong magnetic field. The axion-to-photon conversion is governed by the interaction Lagrangian [3]:

$$L_{a\gamma\gamma} = g_\gamma \frac{\alpha}{\pi} \frac{a(x)}{f_a} \vec{E} \cdot \vec{B} \quad (2)$$

where \vec{E} is the cavity electric field to be detected from the conversion and \vec{B} is the external magnetic field, α is the fine structure constant, f_a is the axion decay constant, $a(x)$ is the axion field and g_γ is the model-dependent coupling equals to -0.97 and 0.36 in the KSVZ and DFSZ model, respectively [3].

A configuration suitable to maximize this term consist of a large superconducting solenoid and a high Q microwave cavity [11]. Only the mode TM_{010} will appreciably couple because it has an electric field component parallel to the magnetic field (see Eqs. (2) and (3)). The conversion power is proportional to the Q factor when it is bigger than the Q_a factor of axions being in the halo of our galaxy (ratio of their total energy to the energy spread) and is proportional to the volume of the cavity.

The power developed in the cavity due to the resonant axion-photon conversion is [11]:

$$P = \left(\frac{\alpha g_\gamma}{\pi f_a} \right)^2 \frac{V B_0^2 \rho_a C}{m_a} \min(Q, Q_a) \quad (3)$$

where V is the volume of the cavity, B_0 is the magnetic field strength at the center of the cavity, ρ_a is the density of galactic halo axions at Earth, f is the axion frequency, f_0 is the cavity resonance frequency, and C is a mode-dependent form factor ~ 0.69 [11].

The signal-to-noise ratio for the system is $SNR = (P_0/k_B T_s)(t/B_a)^{1/2}$, where T_s is the system noise temperature, k_B is the Boltzmann constant, t is the integration time, and B_a is the axion bandwidth. The

search of the axion signal is realized by scanning the cavity with discrete tuning steps $f_{step} \sim 2\text{kHz}$ to cover the expected microwave frequencies associated with the axion conversion.

III. Method

Superconducting magnet.- The magnetic field necessary to couple the axions to the electromagnetic field is generated by a superconductive solenoid surrounding the cavity with inner diameter of 60 cm, length of 100 cm and a weight of 6 tons (NbTi wire in a copper stabilizer). It is mounted near the bottom of a cylindrical cryostat and surrounded by a LN_2 cooled radiation shield. The cryostat is 3.5 m tall and 1.3 m in diameter and the LHe above the magnet has a capacity of 400 Lt. as shown in Figure 1. In this configuration the operating field is 7.6 T.

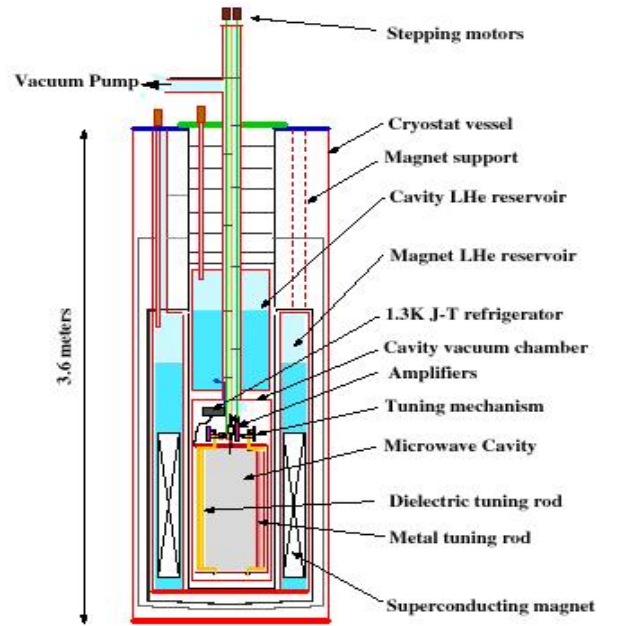


Fig. 1. Cryostat, Magnet and the microwave cavity.

Microwave cavity.- The microwave cavity is made from copper-plated stainless steel and has its own LHe reservoir. By regulating the liquid helium into the vessel the cavity temperature is maintained at 1.3 ± 0.1 K. The resonant frequency of the microwave cavity depends on its size as well as on the position of the tuning elements in the cavity. The cavity is 1 m tall and 50 cm in diameter and it has a frequency range 300-800 MHz. Microwave power is fed into and from the cavity by two semi-rigid coaxial probes. One very weakly coupled (minor) port is used to inject power to measure the cavity transmission and frequency, the second critically coupled (major) port is used to couple power into the pre-amplifier. The frequency of the TM_{010} mode can be tuned moving a pair of metal or dielectric rods

inside the cavity shown in Figure 2. In this case a rod of copper and another of alumina are used.

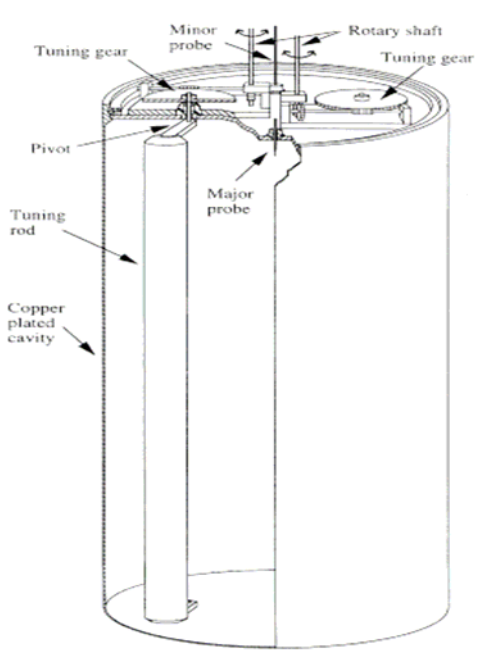


Fig. 2. Cavity with frequency tuning mechanism.

The radial displacement of the copper rod towards the cavity center shifts the TM_{010} frequency up, whereas moving the alumina rod in that direction shifts its down. In this way it is possible to tune the frequency of the cavity. An extra frequency shifting can be obtained by filling the cavity with helium at 1.3 K that changes the dielectric constant causing the form factor C_{010} shifts.

Microwave electronics.- The power from the cavity is coupled to a cryogenic High Electron Mobility Transistor (HEMT) pre-amplifier by an E-field probe that works as an antenna to collect the power from the cavity with noise temperature ~ 1 -2 K and power gain of ~ 15 dB. The preamplifier is followed by a room temperature amplifier and the signal is mixed with a local oscillator (LO) to get an intermediate frequency (IF) at 10.7 MHz. Then two more IF amplifiers are employed before a band-pass crystal filter of bandwidth of 30 kHz. These are followed by another mixing stage consisting on another signal generator as a LO and a balanced mixer [11], shifting the cavity signal to a central frequency of 35 kHz. This down-shifted signal is applied to a real-time 400-point FFT (Fast Fourier Transform) spectrum analyzer with a resolution of 125 Hz. This channel is referred as medium resolution channel, which is appropriate to search for fully thermalized axions ($\Delta E/E \sim 10^{-6}$), where the signal would be distributed over ~ 750 Hz width around 700 MHz [3].

Additionally, the radio signal (35 kHz) is fed to a LO and band-pass filter with a bandwidth of 4 kHz. The filter

output is mixed down to a center frequency of 5.5 kHz and then processed in a computer. After processed, the signal data is analyzed by a FFT power spectrum resulting in a spectrum with resolution of 0.02 Hz. This is called high resolution channel, which is appropriate for the research of fine structure, $\Delta E/E \sim 10^{-11}$. This results from the predicted recent capture of extra-galactic axions by the gravitational potential of our galaxy [11]. A schematic diagram of the microwave detector is shown in Figure 3.

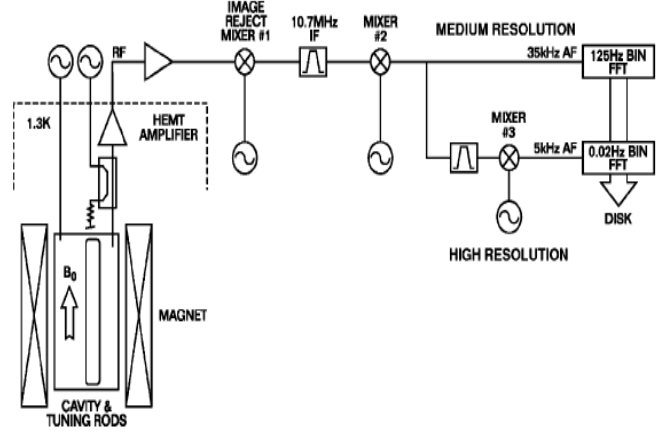


Fig. 3. Schematic Diagram of the axion detector microwave electronics.

IV. Data acquisition and analysis

To minimize systematic errors, at least two global scans over every frequency point are employed. And as the frequency step, $f_{step} \sim 2$ kHz, is much smaller than the receiver bandwidth (~ 30 kHz from the bandwidth of the crystal filter) each frequency is covered ~ 15 times per global scan. Every raw of data consists of the power spectrum from the RF cavity and the experimental parameters; detector sensitivity, cavity resonance frequency and Q factor, the electric coupling of the major port, cavity temperature, B field, microwave background, electronic noise, etc. The excess in power from the cavity is obtained and analyzed from the normalized power spectrum and all the experimental data for a given frequency. Finally, the resonance frequency of the cavity is step-tuned by over ~ 2 kHz and the next cycle begins.

Each raw includes experimental status parameters and a power spectrum from the RF cavity. Each power spectrum contains 400 frequency bins and each bin is 125 Hz in a fixed frequency window of 10-60 kHz. Figure 4 shows a typical power spectrum from the spectrum analyzer where the crystal filter causes falloffs in power outside the bandwidth of 20-50 kHz.

The spectrum used for the analysis is taken from the middle 175 frequency bins of each 400-point spectrum. The final power spectrum from the cavity is normalized and the axion signal would be an excess in this power spectrum.

The candidates to axion signal are those whose power excesses are above certain candidate threshold in units of rms noise floor power σ , depending on the sensitivity of the peak search [3, 11, 12, 13] at a desired confidence level.

The confidence level (CL) of the axion search is obtained by injecting a fake axion-like signal into a Monte Carlo Simulation (MCS). To obtain the relation between the confidence level and the candidate threshold, a signal of an artificial axion with Maxwellian power distribution, specified power and known frequency is injected into a raw data in the MCS. The percentage of the injected fake signals identified in the peak search gives the CL at a certain threshold.

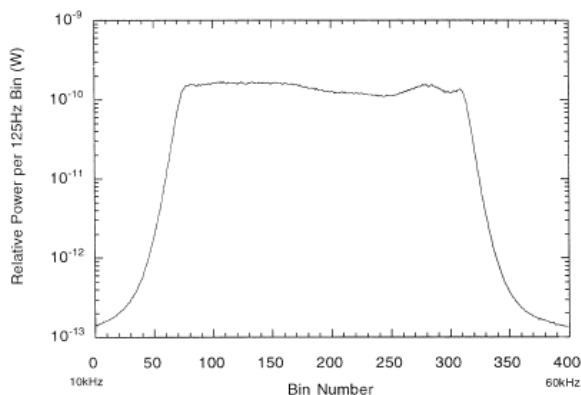


Fig. 4. Typical power spectrum from the spectrum analyzer.

Exclusion process.- The axion search exclusion process has four stages from scanning frequency points to establishing exclusion limits as explained in Ref. [11]. In the first stage, the cavity frequency is tuned step by step over a wide frequency region. For every frequency region two or more scans are performed to achieve the Signal-to-noise ratio corresponding to the desired CL.

In the medium resolution channel a single bin (125 Hz) and 6 bin (750 Hz) co-added bandwidth are examined separately. To achieve a final CL of 90%, then a CL for the primary scan larger than 90% is required, typically of 92-93% for the 6 bin co-added channel. This is the first axion candidate list generated. In the second stage the candidates resulting from the first stage are scanned (rescan). The signal-to-noise ratio of the rescan is set to be equal or larger than the first primary scan resulting in a confidence level above 99%. In the third stage the surviving candidates require a further scan (persistent candidate scan). At this stage the confidence level to the cut is set to be above 99%. Usually, only a few candidates survive the persistent candidate scan. Nearly all the surviving candidates are found to be strong radio peaks which could be TV or wireless telecommunication signals. At the fourth stage the surviving candidates are

examined by terminating the minor port and the couple port where the external radio signals could couple into the cavity and pre-amplifier in order to identify the candidates being strong radio signals.

If a candidate still survives the radio peak inspection, final examination would be done by determining whether the persistent candidate survive after ramping down the B-field and look for a behavior like $P_0 \sim B^2$ (see Eq. (3)). After this four-stage search, the exclusion limit for the axion can be obtained as the product confidence levels of the various scans.

V. Results

As a result of the development of the cavity, the sensitivity of the instrumentation and the data analysis, the ADMX (Axion Dark Matter Experiment) achieves a power sensitivity better than 10^{-23} W in the mass range 1.9-3.3 μeV . Figure 5 shows the axion halo mass density excluded at greater than 90% CL of thermalized KSVZ and DFSZ axions. There are the results of the experiments in 2003-2004 [12].

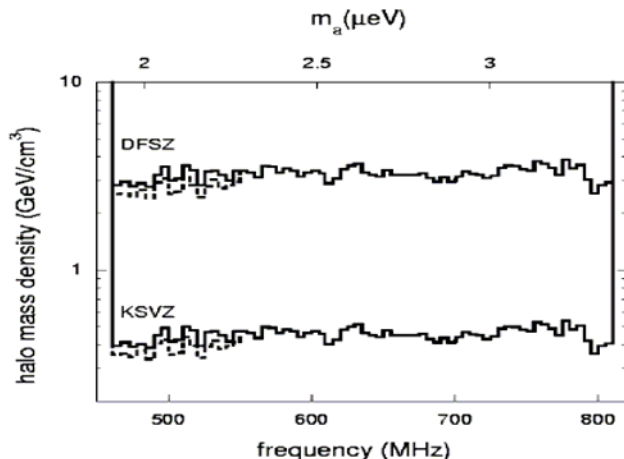


Fig 5. Upper limits on galactic axion dark matter halo mass density excluded at greater than 90% confidence for KSVZ and DFSZ axions.

In 2006 the microwave cavity detector performed a high resolution search for axions, and no axion signals were found in the mass range 1.98-2.17 μeV [13], placing upper limits in the density of axions recently fallen into the halo (non complete thermalized) (see Ref. [3]). Figure 6 shows the newest results of the ADMX experiment.

Future.- To be able to scan at higher frequencies, and then to search for higher axion masses, a pack of four identical smaller cavities, each 20 cm in diameter and 1 m long, can be used [11]. To improve the system noise temperature, an ultra-low temperature design based on SQUID amplifiers and a dilution refrigerator is planned. The HEMT will be replaced by SQUIDS to low the noise. Another possible improvement consists of implementing a cryogenic piezo drive for the tuning rods eliminating the

use of mechanical gears and stepping motors, and then improving the temperature insulation.

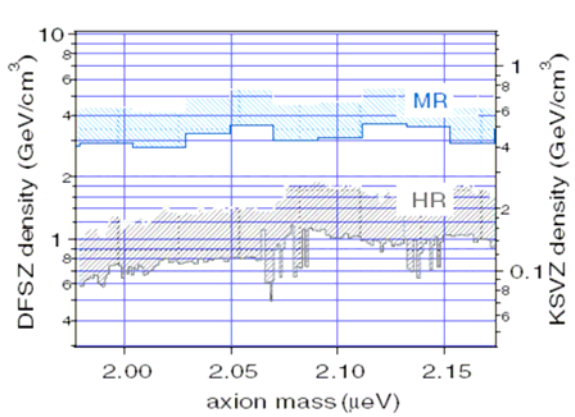


Fig. 6. 97.7% confidence limits for the density of any local axion dark matter flow as a function of axion mass for the DFSZ and KSVZ coupling strengths using the HR channel.

VI. Conclusions

ADMX uses a microwave cavity detector to search for axions in the galactic halo and utilizes the axion electromagnetic coupling to induce resonant conversion of axions to photons. ADMX experiment is the only able experiment to probe realistic dark matter axion models with sufficient sensitivity. In the expected mass range, from 10^{-6} to 10^{-4} eV, the microwave cavity experiments are the most sensitive. Figure 7 shows the sensitivity of many different experiment families. The horizontal axis of the figure shows axion mass, while the vertical axis shows coupling strength. There are two lines marked KSVZ and DFSZ, which represent two different benchmark axion models. The one at the left bottom, which has probed the KSVZ axion model, corresponds to the ADMX experiment.

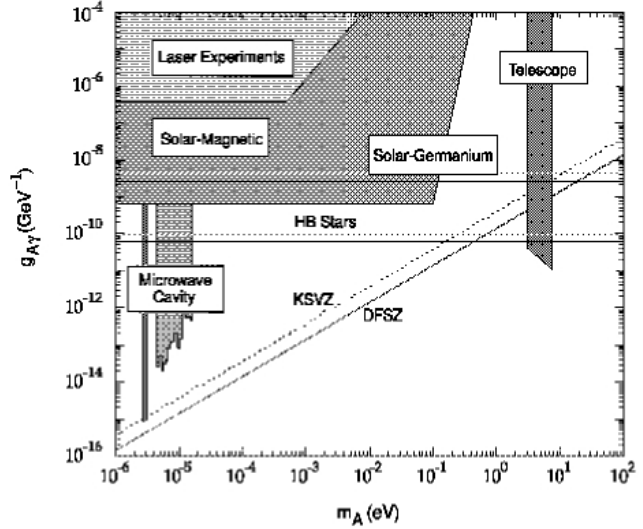


Fig. 7. Sensitivity of different experiments families. The ADMX experiment can test real axion models in the region of axion masses.

REFERENCES

- [1] Pierre Sikivie, Phys.Today 49N12 (1996) 22-27.
- [2] R. D. Peccei, H. R. Quinn, Phys. Rev. D 16, 1791 (1977), Phys. Rev. Lett. 38, 1440 (1977).
- [3] S. Asztalos, et al. Phys. Rev. D 64, 92003 (2001).
- [4] http://pdg.lbl.gov/2006/reviews/contents_sports.html#stanmodeletc
- [5] B. Heckel et al., Phys. Rev. Lett. 97, 021603 (2006).
- [6] A. N. Youdin, et al. Phys. Rev. Lett. 77, 2170 (1996).
- [7] W. T. Ni, et al. Phys. Rev. Lett. 82, 2439 (1999).
- [8] Giles D. Hammond, et al. Phys. Rev. Lett. 98, 081101 (2007).
- [9] G. E. Moody and F. Wilczek, Phys. Rev. D 30, 130 (1984).
- [10] <http://trs-new.jpl.nasa.gov/dspace/bitstream/2014/7471/1/03-1355.pdf>
- [11] Nucl. Instrum. Methods Phys. Res. A 444, 569 (2000).
- [12] S. Asztalos, et al. Phys. Rev. D 69, 11101 (2004).
- [13] L. D. Duffy, P. Sikivie, D. B. Tanner, Phys. Rev. D 74, 12006 (2006).